

Research Article

Structure Optimization of Carbon Nanotubes Based on Swarm Intelligence Algorithm and Evolutionary Computation

Defei Liu 

Center for Studies of Education and Psychology of Ethnic Minorities in Southwest, Southwest University, Beibei, 400715 Chongqing, China

Correspondence should be addressed to Defei Liu; swldf@mau.edu.mk

Received 23 March 2022; Revised 22 June 2022; Accepted 4 July 2022; Published 5 August 2022

Academic Editor: Awais Ahmed

Copyright © 2022 Defei Liu. This is an open access article distributed under the Creative Commons Attribution License, which permits unrestricted use, distribution, and reproduction in any medium, provided the original work is properly cited.

Swarm intelligence algorithm is an emerging evolutionary computing technology, which has become the focus of more and more researchers. It has a very special connection with artificial life, especially evolutionary strategies and genetic algorithms. The swarm intelligence algorithms you see include genetic algorithm, particle swarm optimization algorithm, and ant colony algorithm. This part of the content has been supplemented in the article. Evolutionary computing is a group-oriented random search technology and method produced by simulating the evolutionary process of organisms in nature. Evolutionary computing is based on natural selection strategy: survival of the fittest, elimination of the unfit, and individuals with large fitness values have a higher survival probability than individuals with small fitness values. The purpose of this paper is to study the structure optimization of carbon nanotubes based on swarm intelligence algorithm and evolutionary computation. It is expected to optimize the structure of carbon nanotube materials with the help of intelligent evolution algorithm, so that it can be used in more fields. In this paper, the preparation process and principle of carbon nanotube-based gas sensors are studied, and the preparation process of the side-heated gas sensor is selected. This paper focuses on the strain sensing performance of carbon nanotubes, analyzes various parameters that characterize the sensing performance, and proposes feasible technical routes for improvement, optimization and improvement. The experimental results in this paper show that when different proportions of oxides are added, the tensile strength of carbon nanotube materials is increased by about 8%, and the elastic modulus is increased by up to 40%. After adding CNFs, the tensile strength increased by up to 18%, and the elastic modulus increased by up to 50%.

1. Introduction

With the continuous advancement of science and technology, polymer materials are more and more widely used in daily life, and with the high requirements for the performance of polymer materials, this problem was not solved until the emergence of nanopolymers. Polymer materials are materials based on polymer compounds, materials composed of compounds with relatively high molecular weight, including rubber, plastics, fibers, and polymer-based composite materials. Polymers are the form of life. In fact, every advance of human society is closely related to the development of new materials. In the 21st century, with the continuous development of science and technology, the

understanding of human beings is constantly expanding, and the exploration of nanomaterials has promoted the development of human beings in a deeper direction. Since the end of World War II, optimization computing has been widely introduced and used in the scientific community. Since optimization algorithms already have the advantage of effectively dealing with complex problems that are difficult to solve by traditional methods, these algorithms and designs are sought after as soon as they are published. The optimization algorithm can use the mathematical modeling method to convert the actual problem into an optimization problem and convert the optimization problem into a standard optimization model. It has a simple structure and flexible calculation and can solve many complex problems.

How to combine the swarm intelligence algorithm with evolutionary computing and carbon nanotube structure optimization is the problem to be explored in this paper.

With the increase of function dimension, traditional optimization methods cannot solve complex function optimization problems well. The evolutionary algorithm that simulates the biological evolution process can get a set of solutions in one run. This main advantage is introduced into the optimization problem, which effectively solves many complex optimization problems. The swarm intelligence optimization algorithm has good heuristics, parallelism, and distribution and can solve complex function optimization problems well, save resources, and improve efficiency.

Based on the work of genetic operator impact analysis, this paper proposes GPs based on edit distance 1 and 2 population diversity control, respectively. The influence of genetic operators in GP on the population and its diversity is analyzed and compared, and the correlation between population diversity and individual fitness is explored.

2. Related Work

With the development of the times, more and more people conduct research on optimization calculation. Bhattacharjee and Sarmah attempt algorithmic advantage to solve combinatorial problems. In the improved version of CSA, the local randomized wandering repair operator is used. And in the improved version of FA, variable distance shifts for local search are applied. The firefly algorithm is proposed by simulating the natural phenomenon of firefly swarming activities in nature at night. In the swarming activities of fireflies, each firefly communicates with its companions for food and courtship by emitting fluorescein. The efficiency of the proposed algorithm is demonstrated through experiments using a large number of benchmark problem examples [1]. Ntouni et al. proposed a robust iterative optimization algorithm based on standard particle swarm optimization (PSO) techniques called acceleration-assisted PSO (A-APSO). He implemented the A-APSO algorithm to evaluate the detector weights. The results show that the error performance is better than the weight values evaluated by the PSO algorithm when A-APSO weights are used [2]. Gao et al. proposed a protein structure prediction method. He used three different structural evolution methods, including an improved particle swarm optimization (PSO) algorithm, random perturbation, and fragment replacement, to update the protein structure while keeping the secondary structure unchanged. The high success rate and the accuracy of the results demonstrate the reliability of the method [3]. Zhong et al. proposed to extend the multidimensional similarity space region with group similarity and firstly used the optimal value of the iterative clustering function as the clustering quality index. In addition, he also proposed the fuzzy high-order hybrid clustering (F-HOHC-SIS) algorithm, which can effectively control the convergence speed and reduce the computation time, while improving the anti-interference capability [4]. In cloud environments, various meta-heuristics can be used to solve scheduling problems that fall under the NP-complete problem. Two of the funda-

mental goals of computer science are to discover algorithms that can be shown to perform well and yield optimal or suboptimal solutions. Heuristics, on the other hand, try to provide one or all goals at a time. Tabaghchi proposes task scheduling algorithms to reduce the idle time of virtual machines while achieving load balancing and reducing the running time. According to the results obtained, he reduced the manufacturing time and energy consumption using the proposed algorithm [5]. Son et al. proposed an optimization method to design radar absorbing structures made of fiber-reinforced plastic structures. In the optimized design, the objective function is set to maximize the absorption bandwidth of the X-band stealth. The results confirmed that using the S-FSM not only the electromagnetic performance of the samples could be detected but also the defects caused by the manufacturing process [6]. Ahmadi et al. describe the optimization of parameters involved in the production of nanofibers. Single-walled carbon nanotubes were used to improve the mechanical properties. The results show that the concentration has a greater effect on the fiber diameter than other parameters in PAN and PAN/CNT nanofibers. However, excessive CNTs have a negative effect on elongation and modulus due to the aggregation of CNTs within the nanofibers. The results showed that the PAN nanofibers have an amorphous structure compared to the conventional PAN nanofibers [7]. Lu et al. proposed carbon nanotube bucky paper as a sensing layer in composite materials. Bucky paper is a special kind of carbon nanotube thin layer, which looks very similar to ordinary carbon fiber paper. People also call it "Bucky paper." It is made of only one-fifty thousandth of a human hair, made of molecular weight. The experimental results show that the resistance temperature coefficient of the bucky paper is related to the curing behavior of the resin, and a critical value of the resistance temperature coefficient is determined. In addition, by monitoring and optimizing the curing parameters, the properties of the composites can indeed be improved [8]. Although these theories have analyzed the optimization calculation and carbon nanotube structure to a certain extent, the combination of the two is insufficient and not practical.

3. Swarm Intelligence Algorithm and Evolutionary Computation for Carbon Nanotube Structure Optimization Methods

3.1. Overview of Carbon Nanotubes. Since the 1990s, carbon nanotubes have been paid attention to by scientists. Unlike other materials, carbon nanotubes have two different structures, so carbon nanotubes have many applications in many fields. Carbon nanotubes have two structures, single-walled carbon nanotubes, and multiwalled carbon nanotubes. Single-walled carbon nanotubes can be regarded as hollow cylinders made of a layer of graphite curled, while multiwalled carbon nanotubes are composed of a group of coaxial graphene. In the development of carbon nanometers, its electrical properties have received extensive attention [9, 10]. Nanomaterials are materials with nanoscale structures, which can be divided into zero-dimensional

nanomaterials and one-dimensional nanomaterials according to their specific dimensions. It has been asserted that when people can arrange and combine substances on a very small scale, they will obtain various novel materials [11, 12]. The change in properties caused by the ratio of the number of atoms on the surface of the particle to the total number of atoms increases sharply as the particle size decreases. For example, when the particle diameter is 10 nm, the particle contains 4000 atoms, and the surface atoms account for 40%; when the particle diameter is 1 nm, the particle contains 30 atoms, and the surface atoms account for 99%. Nanomaterials have attracted attention as a potential dielectric material, and most of the current research on this material focuses on the effect of nanoceramic doping on the dielectric properties of ceramics [13]. The electronic properties of metallic carbon nanotubes are not sensitive to the chemical environment, but its electrical conductivity is very superior. It can be used as a wire, and its electrical conductivity far exceeds that of copper, while the internal electronic properties of semiconducting carbon nanotubes are affected by the environment and other substances. In the traditional manufacturing process, the oxide surface is usually coated on the ceramic surface by chemical means. This method can reduce the loss and increase the energy storage density, but since the oxide is a nonferroelectric, the ferroelectric properties of the ceramic itself will interfere [14, 15]. In order to meet the use of nanomaterials in defense and communication, we usually incorporate dopants into the original materials to modify their defects. This method has a good effect and has been widely used in the storage field. In use, it is found that when the doping substances reach a certain limit, the dielectric and ferroelectric properties of ceramics will exhibit relaxation ferroelectric phenomena [16, 17]. The application of nanoceramic materials in capacitors requires a stable dielectric temperature. This is achieved by adding rare earth elements. This method can inhibit the growth of crystal grains and can also obtain dense and fine powders. Figure 1 is an image of nanopowders. This material can be fired into high-density ceramics [18, 19].

Until the end of the last century, the first International Conference on Nanoscience and Technology was held in the United States, which formally combined theoretical research with contemporary science and technology, marking the official birth of nanotechnology [20]. When the size of the material is at the nanometer level, the number of atoms on the surface of the material will increase dramatically, which will far exceed the number of ordinary materials, and the chemical activity of the material will be greatly increased at this time. At the same time, nanomaterials are equal to or smaller than the wavelength of light wave, de Broglie wavelength, and coherence length of superconducting state, and the periodic boundary of the material is destroyed, resulting in “novel” optical, electrical, magnetic, acoustic, and thermodynamic properties. In addition, nanomaterials also have quantum size effects and macroscopic quantum tunneling effects. These unique characteristics provide conditions for the wide-scale application of nanomaterials. With the continuous and in-depth development of theory and practice, nanostructures that are not called sys-

tems have been established. With the maturity of application, the uniqueness of nanomaterials plays a pivotal role in the fields of biotechnology and advanced manufacturing. Figure 2 is a schematic diagram of common nanomaterials.

3.2. Overview of Optimization Calculations. With the continuous development of the production economy, the scale of computation involved is increasing, especially in the fields of management and engineering. With the continuous development of computer technology, and in order to reduce the complexity of the calculation, the optimization calculation came into being. In essence, optimization refers to the use of certain rules to meet the needs of users.

Evolutionary computing is a stochastic optimization method that simulates the genetic mechanism of the animal kingdom. It has the idea of “survival of the fittest.” Therefore, when using evolutionary thinking to solve target optimization problems, genetic operations and natural selection become its important components. Evolutionary algorithms iteratively generate multiple solutions to each problem during the optimization process and continue to generate better solutions. The optimization function is called the fitness function. Each solution is called an individual, and all individuals in each generation form a group. The fitness value of individuals in each group is different. With iteration, better individuals are obtained through certain evolutionary strategies, such as crossover and mutation. When the algorithm terminates, the individual with the best fitness value in the entire population is selected as the solution to the problem. Figure 3 shows the basic structure of the optimization calculation.

Evolutionary algorithm is a random search method. Compared with other enumeration techniques and heuristic search techniques, the global optimal solution probability of this problem is higher. The evaluation information of the objective function is used to make it actionable and general. It is concise in form, can be operated with massively parallel computers, and can be easily combined with other methods. At present, evolutionary computing mainly includes genetic algorithm, evolutionary strategy, and evolutionary planning. Genetic algorithm refers to the population of solution sets, and the population is composed of several individuals encoded by genes. In essence, genetic algorithm is an optimization algorithm, which is a random search algorithm that uses the idea of natural selection and biological evolution to search for the optimal solution in the search space.

$$\min \{g(a) | a \in Q\}. \quad (1)$$

Formula (1) represents the function expression of the function optimization model, where a represents the decision variable, $g(a)$ represents the objective function, and Q represents the spatial subset.

$$\min g(a).st * p(a) \geq 0. \quad (2)$$

Formula (2) represents the decision variable inequality.

$$Q = \{a \in W^s | p(a) \geq 0\}. \quad (3)$$

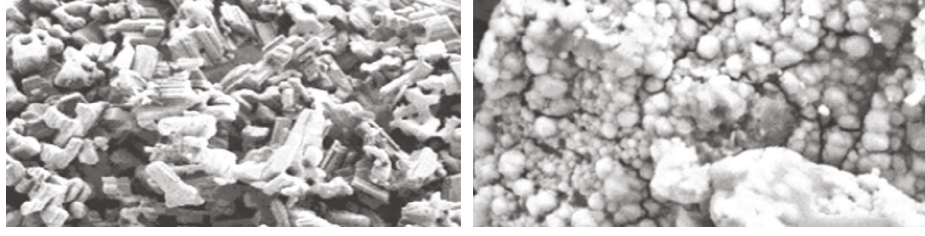


FIGURE 1: Nanopowder image.

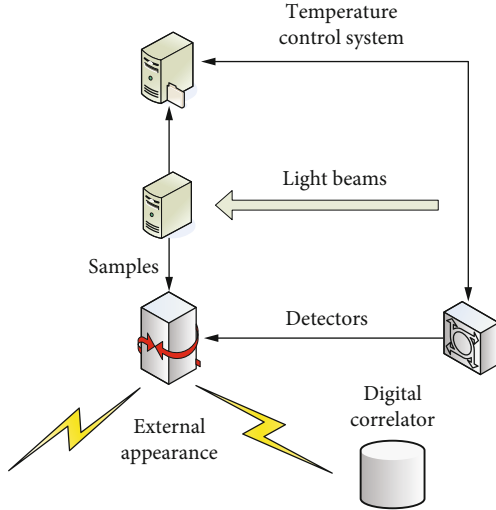


FIGURE 2: Common nanomaterial quiz structure.

Formula (3) represents the feasible region of the decision solution, which is the set of all solutions in layman's terms.

In order to get the optimal solution for the region, we need to optimize the model.

$$\forall a \in QI \left\{ a \in W^s \left| \sqrt{\sum (a_1 - a^*)^2} < a \right. \right\}. \quad (4)$$

When formula (4) is satisfied $g(a^*) \leq g(a)$, we say that the model has an optimal solution. Figure 4 shows the basic flow structure of the algorithm.

$$\beta = \frac{T_{\max} - T_{\min}}{2^p - 1}. \quad (5)$$

Formula (5) represents the precision of binary encoding, among them, T represents the range of values, and p represents the length of the encoded symbol.

$$k = T_{\min} + \left(\sum_{o=1}^p w_o * 2^{o-2} \right) * \frac{T_{\max} - T_{\min}}{2^p - 1}. \quad (6)$$

Formula (6) represents the decoding function expression when the encoded length is k .

$$\begin{cases} f_p = w_p, \\ f_p = w_{p+1} \oplus w_p, \end{cases} \quad (7)$$

$$\begin{cases} w_p = f_p, \\ w_p = w_{p+1} \oplus f_p. \end{cases} \quad (8)$$

Formulas (7) and (8) represent binary codes under different Gray codes.

In the genetic algorithm, we usually use the fitness function to judge the situation of the individual. The fitness function satisfies the generality, so the calculation steps can be reduced in the actual use process.

$$\text{Fitness}(g(a)) = g(a). \quad (9)$$

Formula (9) represents the functional expression of the maximal optimization problem.

$$\text{Fitness}(g(a)) = -g(a). \quad (10)$$

Formula (10) represents the functional expression for the minimal optimization problem.

Computers have been developing and progressing continuously since their appearance in 1946 and have been fully used in various fields of social production. Although the development is very rapid, the production needs of human beings are also expanding, and the traditional computing performance cannot meet the current development needs, so high-performance computing came into being. With the ever-increasing demand for computing power, high-performance computing is also evolving. The current research directions of high-performance computing include cluster computing, network computing, cloud computing, and FPGA-based reconfigurable heterogeneous computing [21]. The initial high-performance computing focused on the computing field, but with the continuous improvement of high-performance computing, high-performance computing has basically become an essential means of research, and high-performance computing can be seen in various fields. From computers, minicomputers to mainframes, the development and replacement of computers are fast, but they still cannot meet the needs of computing. Scientific computing, network computing, terminal computing, cloud computing, supercomputing, intelligent computing, GPU computing

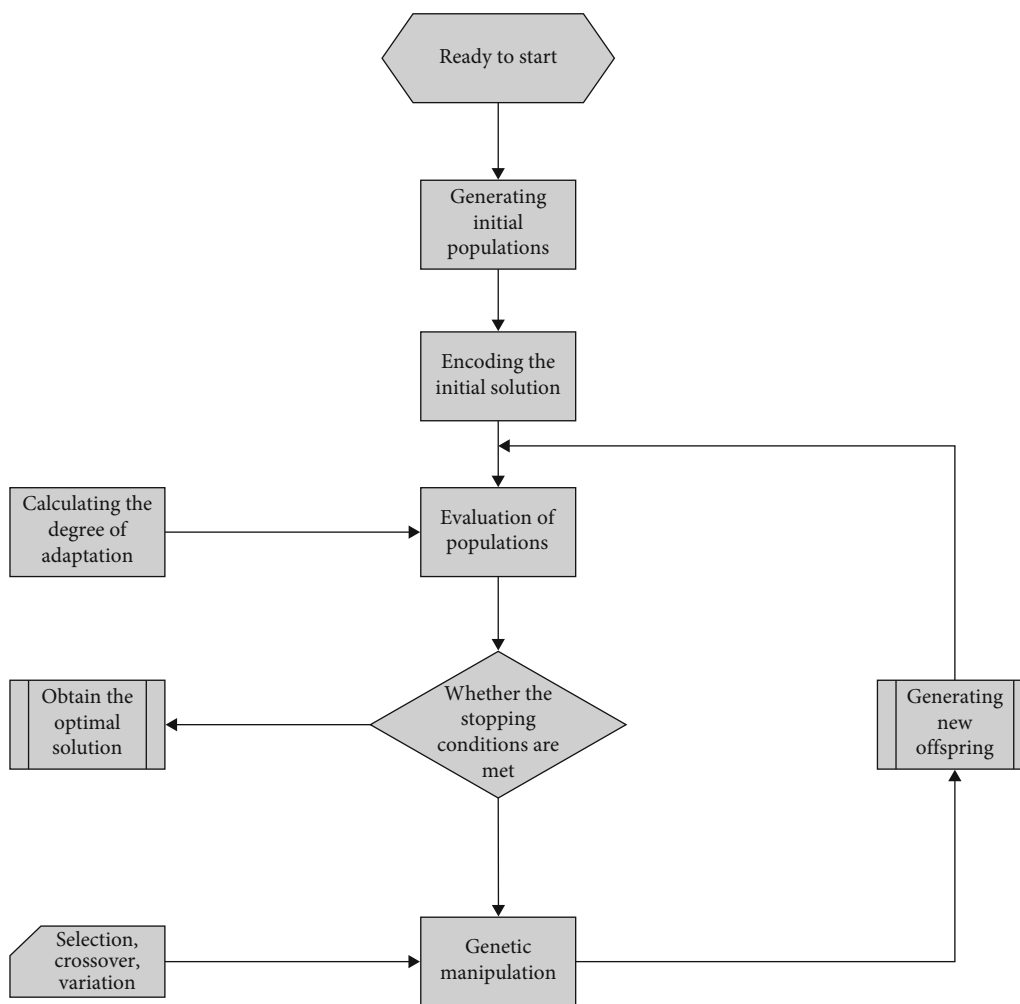


FIGURE 3: Basic framework of genetic algorithm.

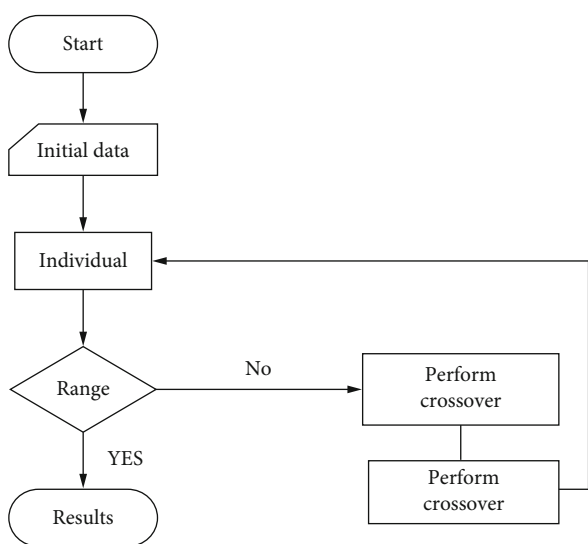


FIGURE 4: Model algorithm flow demonstration

and other computing modes, concepts, technologies, and applications dominate the progress and development of science and technology. Quantum computing, brain-like computing, borderless computing, human-machine-object ternary fusion computing, data-intensive computing, etc. have brought computing into the era of diversity. Although high performance computing has many advantages, the issues affecting the development of high performance computing are power consumption, energy efficiency ratio, energy saving, ecological environment and industrialization, performance and scalability, reliability and fault tolerance, application efficiency and applicability, efficient management, and low threshold operation [22, 23].

Figure 5 is a schematic diagram of a high-performance scientific computing cluster architecture.

China's research on high-performance computing is relatively late, and the pace of research has been officially started since the advent of China's first shared storage multiprocessor system. The Dawning 400A, developed in 2004, has entered the top ten in the world in computing power. In 2017, the world's first optical quantum computer that surpassed the early classical computers was born. The successful

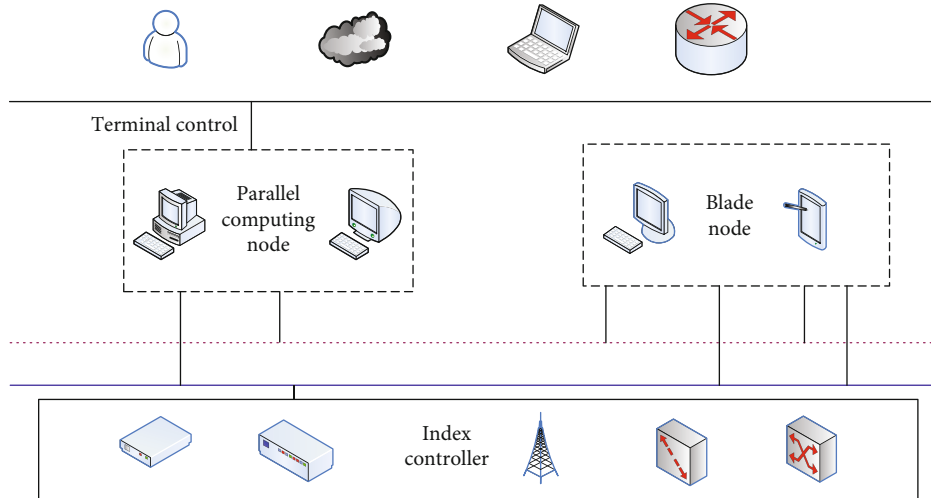


FIGURE 5: High-performance scientific computing cluster architecture.

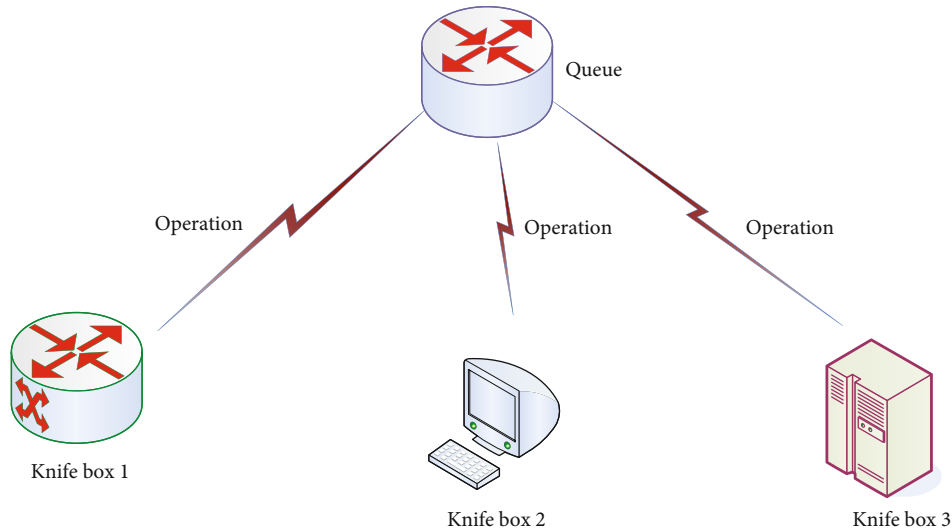


FIGURE 6: High-performance computing architecture.

development of the E-class system in 2018 shows that China’s computing level has entered the forefront of the world and occupies a very important position in the field of high-performance computing. Figure 6 is a schematic diagram of a high performance computing architecture.

GC-MS is an analytical instrument that can obtain a set of chronological data during the experiment. During the experiment, the target object is composed of t parts, then each component is 1, 2, 3 ... n ; the specific function expression is as follows:

$$W_1 = W_{11}, W_{12}, \Lambda W_{1M}, \tag{11}$$

$$W_2 = W_{21}, W_{22}, \Lambda W_{2M}, \tag{12}$$

$$W_N = W_{N1}, W_{N2}, \Lambda, W_{NM}. \tag{13}$$

Among them, W stands for different components.

Introducing the above formula into a matrix, it can be simplified to

$$W = \begin{pmatrix} W_{11}, & W_{12}, & \Lambda & W_{1M} \\ W_{21}, & W_{22}, & \Lambda & W_{2M} \\ \Lambda & \Lambda & \Lambda & \Lambda \\ W_{N1}, & W_{N2}, & \Lambda & W_{NM} \end{pmatrix}. \tag{14}$$

If the matrix is the distribution of n mixtures during the experiment; then, it can be represented by a two-

dimensional matrix. Each row represents a time point, and each column represents the distribution status. The specific function expression is as follows:

$$E = \begin{pmatrix} E_{11}, & E_{12}, & \Lambda & E_{1N} \\ E_{21}, & E_{22}, & \Lambda & E_{2N} \\ \Lambda & \Lambda & \Lambda & \Lambda \\ E_{U1}, & E_{U2}, & \Lambda & E_{UN} \end{pmatrix}. \quad (15)$$

Among them, E represents a two-dimensional matrix.

$$Q_K(C) = \frac{2}{R(c)} \sum_{k=1}^n N_{uk} * Y_{uk}. \quad (16)$$

Among them, Q represents the set of indicators, and $Q_K(C)$ represents the indicators under point C .

$$\alpha(C) = \int_M^1 \left(Q_K(C) - \frac{1}{m} \sum_{k=1}^m Q_K(C) \right)^3. \quad (17)$$

Among them, according to $0 < Q_K(C) \leq 1$, $0 \leq \alpha(C) < 0.57$ can be obtained.

$$\beta(C) = 1 - 2 * \alpha(C). \quad (18)$$

Among them, according to $0 \leq \alpha(C) < 0.57$, $0 \leq \beta(C) \leq 1$ can be obtained.

$$QW_j(c, r) = \frac{1}{\sqrt{c}} \int_{-\infty}^{+\infty} j(r)\chi * \left(\frac{w-t}{c} \right) dw. \quad (19)$$

Among them, $QW_j(c, r)$ is the wavelet coefficient, $\chi(w)$ is the wavelet basis function, and $j(r)$ is the analysis signal.

$$L_V = W \text{diag} \left(s_{(v)} \right) D^U + Q_v, \quad v = 1, 2, \Lambda, V. \quad (20)$$

Among them, L stands for cubic matrix, W stands for pure chromatogram, and D stands for pure mass spectrum.

4. Swarm Intelligence Algorithm and Evolutionary Computation for Carbon Nanotube Structure Optimization Experiment

4.1. Experimental Material Parameters. Materials are the material basis for human survival and the symbol of human material civilization. Materials are the backbone of modern science and technology. At the same time, the progress of science and technology has put forward higher requirements for materials. The structural optimization of carbon nanotube materials explored in this paper is expected to bring infinite possibilities for development through the optimization of material structure. The material parameters involved in this paper are as follows.

TABLE 1: Mechanical parameters of composite materials.

Grain size	Volumetric fraction 6%			Volumetric fraction 10%		
	A (GPa)	B (GPa)	c	A (GPa)	B (GPa)	c
10	4.52	1.68	0.32	5.23	1.93	0.35
11.3	4.47	1.65	0.31	5.22	1.9	0.35
12.4	4.45	1.65	0.32	5.2	1.87	0.33
13.24	4.43	1.63	0.32	5.17	1.85	0.34
14.8	4.4	1.61	0.31	5.13	1.83	0.33

TABLE 2: Nanoparticle unit cell elastic stiffness matrix.

Z (GPa)	1	2	3	4	5
1	6.98	5.32	5.01	-0.31	-0.05
2	7.63	6.31	5.21	-0.04	1.37
3	6.31	4.74	6.97	1.43	0.39
4	5.02	5.25	3.28	0.41	1.39
5	-0.41	-0.03	-0.15	0.039	0.52

TABLE 3: Matrix action energy.

Grain size	Volume	Energy is 5%	Energy is 10%	5% energy per unit volume	10% energy per unit volume
10	4258	-304	-402	-0.09	-0.015
11.27	6512	-501	-456	-0.08	-0.06
12.3	7365	-536	-526	-0.07	-0.03
13.2	8964	-648	-614	0.06	-0.054
14.1	10254	-712	-715	-0.043	0.048

TABLE 4: Single cell model and single cell mechanical properties.

Performance	PI	Volumetric fraction 5%	Volumetric fraction 10%
Young's modulus	4.15	4.6	4.79
Volume	5.4	5.87	7.43
Lamé constant	4.62	4.71	6.25
Shear modulus	1.53	1.63	1.71
Poisson's ratio	0.35	0.36	0.37

As can be seen from the data in Table 1, assuming that the diameter of the nanoparticles is 10 nm and the thickness of the interface layer is 10 nm, when the volume of the nanoparticles increases continuously, the elastic modulus of the material will also change and show a certain linear law. When the diameter of the nanoparticle is 11.3 nm and the volume fraction is 6%, its elastic modulus is 0.31, and when the volume fraction is 10%, its elastic modulus is 0.35. When the diameter of the nanoparticle is 12.4 nm and the volume fraction is 6%, its elastic modulus is 0.32, and when the volume fraction is 10%, its elastic modulus is 0.33. When the diameter of the nanoparticle is 13.24 nm and the volume

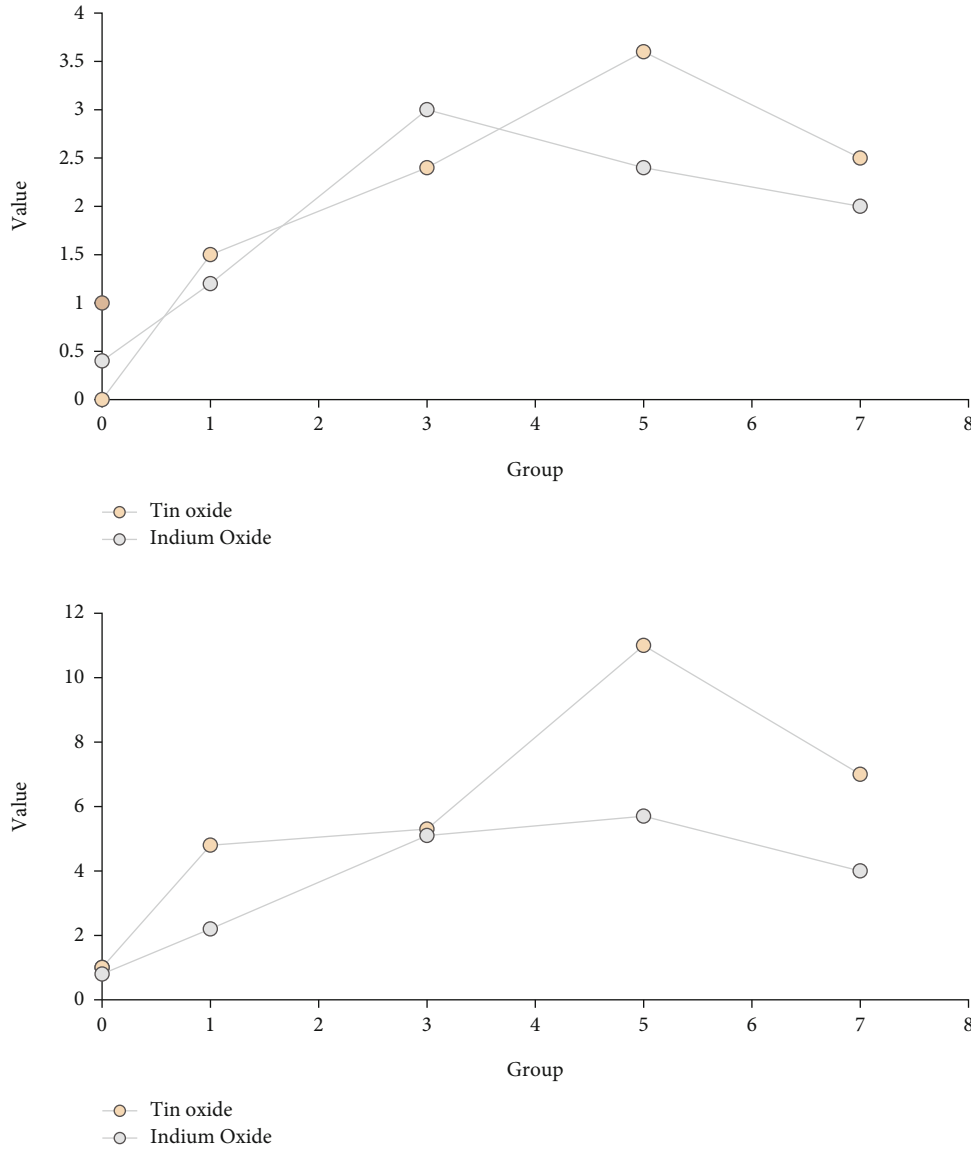


FIGURE 7: Doping concentration vs. sensitivity curve of carbon nanotubes.

fraction is 6%, its elastic modulus is 0.32, and when the volume fraction is 10%, its elastic modulus is 0.34. When the diameter of the nanoparticle is 14.8 nm and the volume fraction is 6%, its elastic modulus is 0.31, and when the volume fraction is 10%, its elastic modulus is 0.33. According to the data, when the particle diameter increases, the elastic modulus decreases and the change trend is relatively gentle.

According to the data in Table 2, there are many factors that affect carbon nanomaterials, and anisotropic materials are used in the experiment. However, according to the data in Table 2, the values of many materials can be regarded as zero, and there are also many materials whose values are relatively close under certain conditions. In fact, when determining the range of particle variation, the number of atoms increases at a certain rate, and when the volume fraction of nanoparticles is 6%, the number of unit cells

surges, and the number of filled molecular chains also increases rapidly.

4.2. Correlation between Material Structure and Matrix. Nanocomposites consist of filler particles, a polymer matrix, and an interface between the two. In order to explore the relationship between the properties and energy of nanomaterial structures, it is necessary to perform single-point energy calculations to obtain the interaction energy between the two.

According to the data in Table 3, when the nanoparticles embedded in the unit cell are enlarged, the number of atoms around them will also increase, and the number of non-bonded pairs between the nanomaterial structure and the matrix will also increase, so the interaction between the two also increases. When the diameter of the material is 10 nm and the volume is 4285, the energy ratios are -0.09

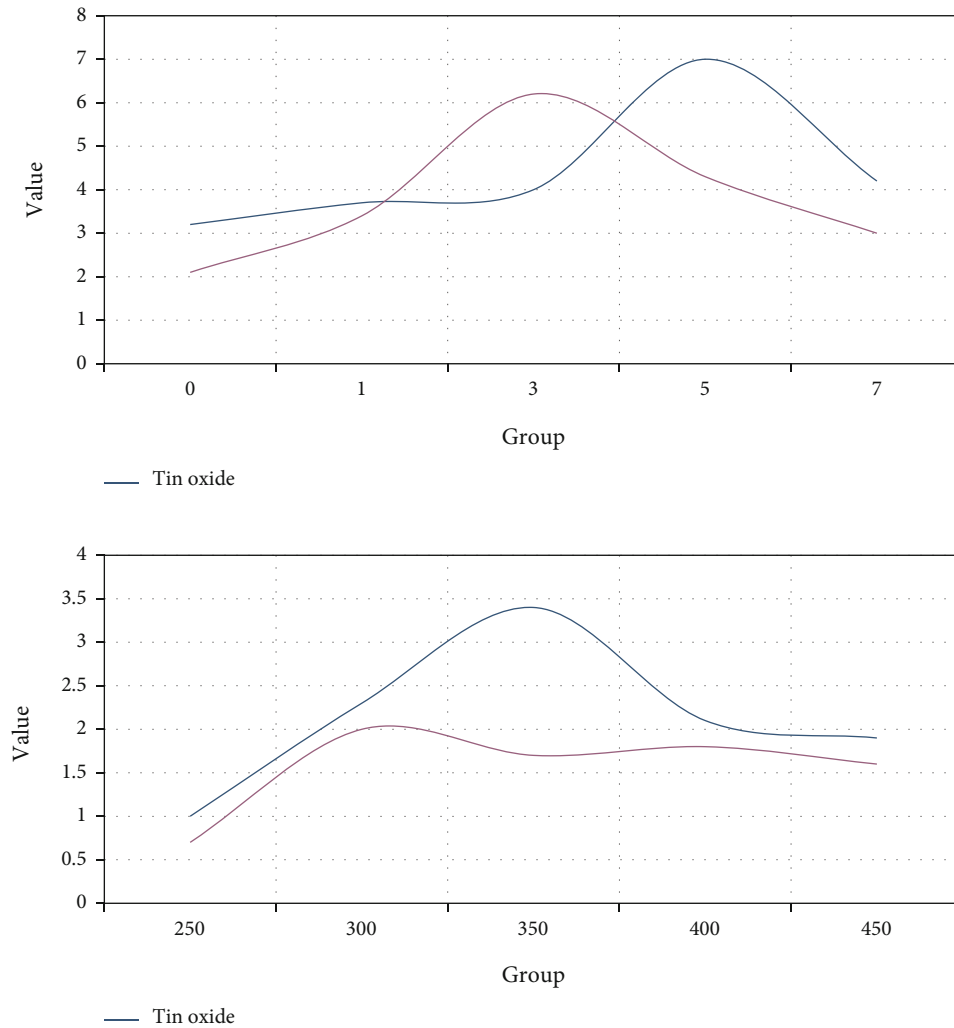


FIGURE 8: Curves of operating temperature versus sensitivity.

and -0.015 in different cases, respectively. When the diameter of the material is 11.27 nm and the volume is 6512, its energy ratios are -0.08 and -0.06 under different conditions, respectively. When the material has a diameter of 12.3 nm and a volume of 7365, its energy ratios are -0.07 and -0.03 under different conditions, respectively. When the diameter of the material is 13.2 nm and the volume is 8964, its energy ratios are 0.06 and -0.054 under different conditions, respectively. When the diameter of the material is 14.1 nm and the volume is 10254, its energy ratios are -0.043 and 0.048 under different conditions, respectively. According to this data, the qualitative correlation between the elastic properties of nanomaterials and the action energy is also related to the volume of nanoparticles. When the diameter of nanoparticles increases, the body-to-surface ratio decreases, resulting in a decrease in the number of nonbonded pairs, weakening the interaction energy, and reducing the elastic modulus of the composite.

4.3. Single-Cell Model and Single-Cell Mechanical Properties. Combined with molecular dynamics, this experiment simu-

lates the mechanical properties of nanomaterials, explores the effects of nanoparticles and volume, and explores the relationship between the number of nanoparticles and the properties of composite materials.

According to the data in Table 4, when the PI of the nanomaterial is 4.15 and the volume fraction is 5%, the Young's modulus of the material is 4.6, and when the volume fraction is 10%, the Young's modulus of the material is 4.79. When the PI of the nanomaterial is 5.4 and the volume fraction is 5%, the Lamé constant of the material is 4.71, and when the volume fraction is 10%, the Lamé constant of the material is 6.25. When the PI of the nanomaterial is 1.53 and the volume fraction is 5%, the shear modulus of the material is 1.63, and when the volume fraction is 10%, the shear modulus of the material is 1.71. When the PI of the nanomaterial is 0.35 and the volume fraction is 5%, the Poisson's ratio of the material is 0.36, and when the volume fraction is 10%, the Poisson's ratio of the material is 0.37. According to this data, the Young's modulus, shear modulus, Lamé constant, and volume of the composites all increased when nanoparticles were added to the material.

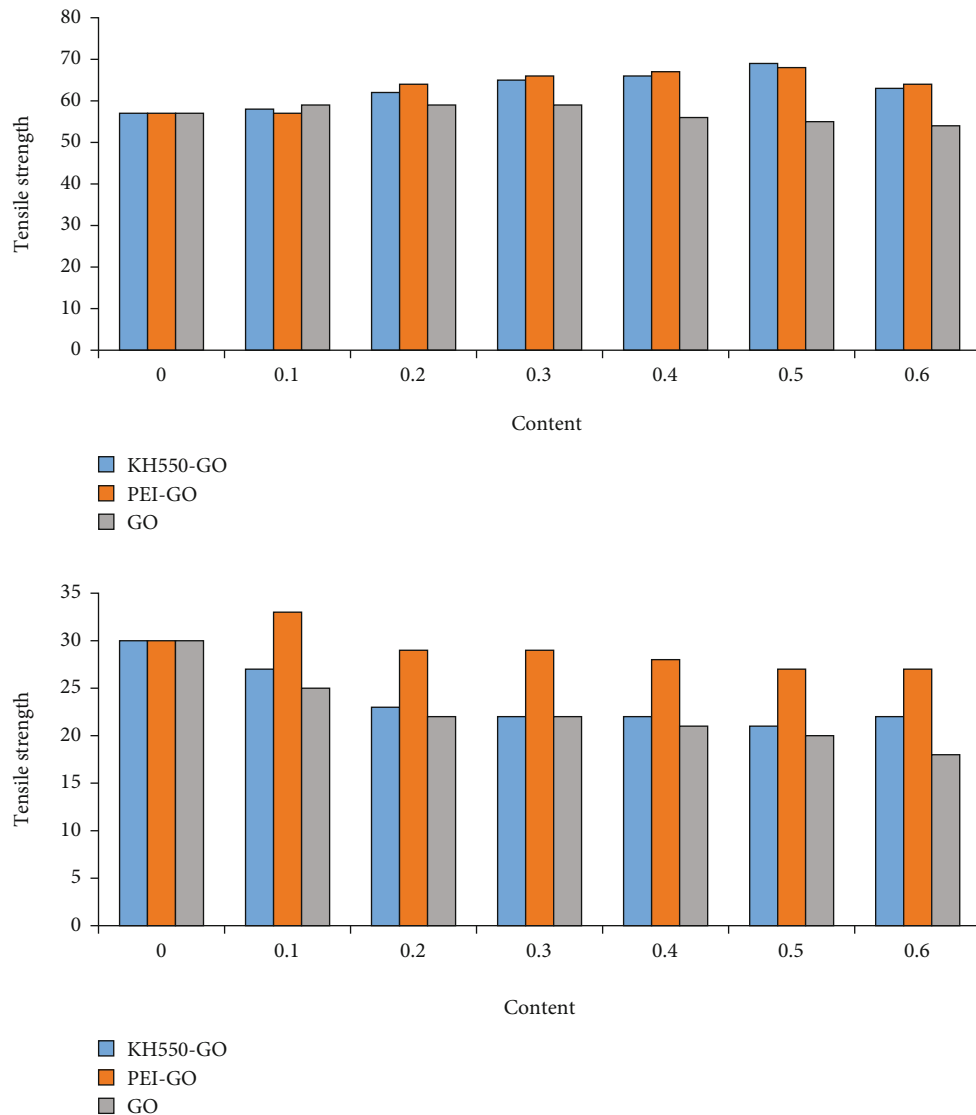


FIGURE 9: Schematic diagram of the secondary mechanical properties of the composite material.

And the data show that the difference becomes more obvious with the increasing volume, but the Poisson's ratio does not change much.

5. Swarm Intelligence Algorithm and Evolutionary Computation for Structure Optimization of Carbon Nanotubes

5.1. Gas Sensitivity of Carbon Nanotubes. Sensors are an important tool in modern technology. Gas sensitivity is an important branch of sensors that can detect different gases. Therefore, gas sensors are widely used in food and medical fields. Based on this, in order to find out the optimal doping concentration of carbon nanotubes for the two metal oxides, we analyzed them as follows.

According to the data in Figure 7, in order to explore the doping concentration of carbon nanotubes to different oxides, we analyzed the nanomaterials at different tempera-

tures. When the experimental temperature is 150 degrees Celsius, the sensitivity of tin oxide is 0, and the sensitivity of indium oxide is 0.4 in the case of dopant. When the doping content of tin oxide is 1%, the sensitivity of the sensor is 1.5, and when the doping content of indium oxide is 1%, the sensitivity of the sensor is 1.2. When the doping content of tin oxide is 3%, the sensitivity of the sensor is 2.4, and when the doping content of indium oxide is 3%, the sensitivity of the sensor is 3. When the doping content of tin oxide is 5%, the sensitivity of the sensor is 3.6, and when the doping content of indium oxide is 5%, the sensitivity of the sensor is 2.4. When the doping content of tin oxide is 7%, the sensitivity of the sensor is 2.5, and when the doping content of indium oxide is 7%, the sensitivity of the sensor is 2. According to the data, when the doping content of tin oxide is 5%, the sensitivity of the sensor is the best, and when the doping content of indium oxide is 3%, the sensitivity of the sensor is the best.

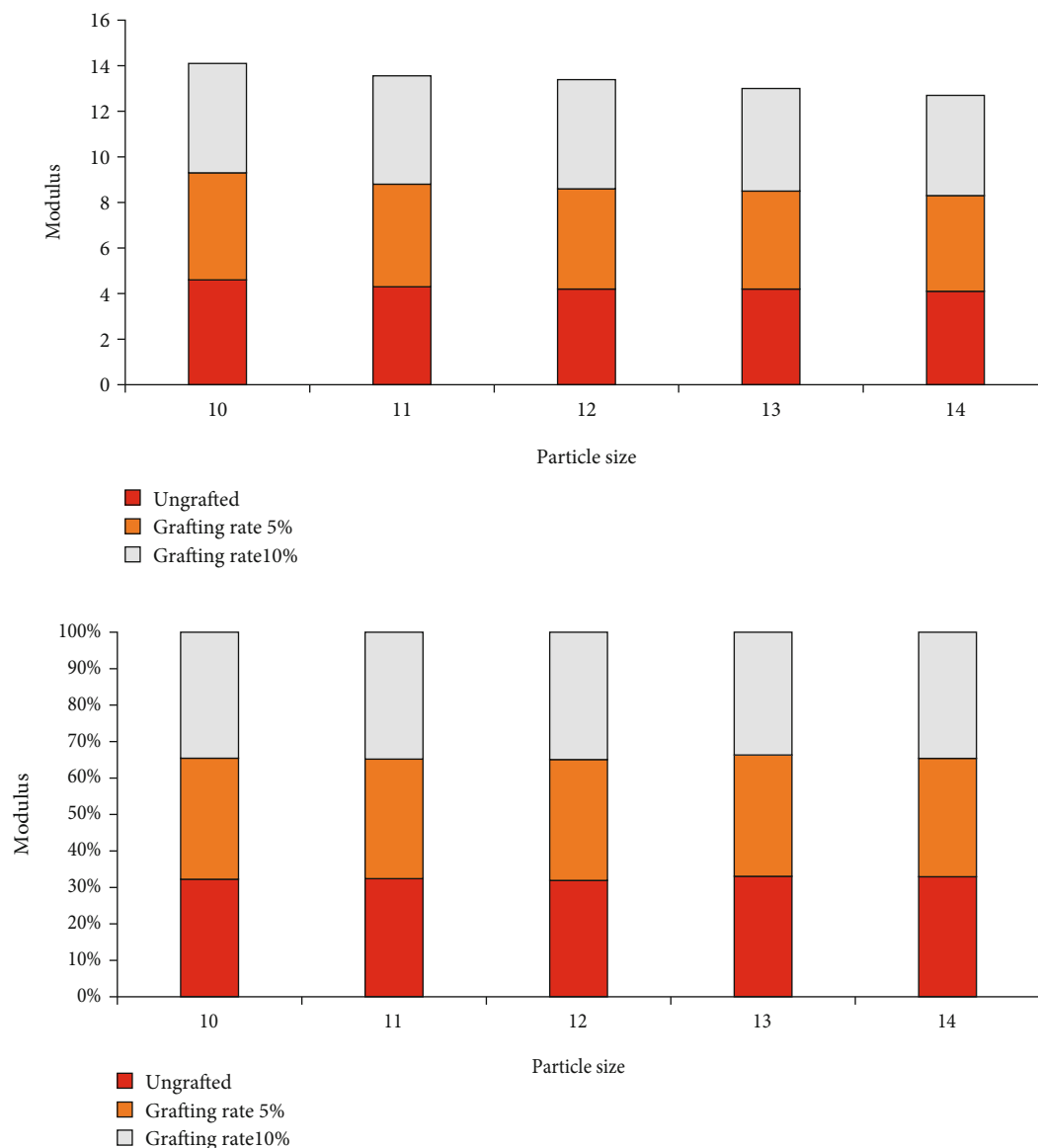


FIGURE 10: Schematic diagram of the relationship between composite material modulus and particle size.

When the experimental temperature is 250 degrees Celsius, in the case of dopant, the sensitivity of tin oxide is 1, and the sensitivity of indium oxide is 0.8. When the doping content of tin oxide is 1%, the sensitivity of the sensor is 4.8, and when the doping content of indium oxide is 1%, the sensitivity of the sensor is 2.2. When the doping content of tin oxide is 3%, the sensitivity of the sensor is 5.3, and when the doping content of indium oxide is 3%, the sensitivity of the sensor is 5.1. When the doping content of tin oxide is 5%, the sensitivity of the sensor is 11, and when the doping content of indium oxide is 5%, the sensitivity of the sensor is 5.7. When the doping content of tin oxide is 7%, the sensitivity of the sensor is 7, and when the doping content of indium oxide is 7%, the sensitivity of the sensor is 4. According to the data, when the doping content of tin oxide is 5%, the sensitivity of the sensor is the best, and when the doping content of indium oxide is 5%, the sensitivity of the sensor is the best.

According to the data in Figure 8, when the experimental temperature is 350 degrees Celsius, in the case of dopant, the sensitivity of tin oxide is 3.2, and the sensitivity of indium oxide is 2.1. When the doping content of tin oxide is 1%, the sensitivity of the sensor is 3.7, and when the doping content of indium oxide is 1%, the sensitivity of the sensor is 3.4. When the doping content of tin oxide is 3%, the sensitivity of the sensor is 4, and when the doping content of indium oxide is 3%, the sensitivity of the sensor is 6.2. When the doping content of tin oxide is 5%, the sensitivity of the sensor is 7, and when the doping content of indium oxide is 5%, the sensitivity of the sensor is 4.3. When the doping content of tin oxide is 7%, the sensitivity of the sensor is 4.2, and when the doping content of indium oxide is 7%, the sensitivity of the sensor is 3. According to the data, when the doping content of tin oxide is 5%, the sensitivity of the sensor is the best, and when the doping content of indium oxide is 3%, the sensitivity of the sensor is the best.

According to the experimental data, the sensitivity of carbon nanotubes changes differently at different temperatures. The sensitivity of tin oxide is the best at 350 degrees Celsius, and the sensitivity of indium oxide is the best at 300 degrees Celsius.

5.2. Performance of Carbon Nanotube Materials. According to Figure 9, the tensile strength, elongation, and Young's scale of the original nanomaterials all decreased to varying degrees, mainly due to the structural defects induced by the agglomerates in the matrix, resulting in a decrease in the mechanical energy of the nanomaterials. The improved agglomerates show an initial decrease in energy, allowing them to be more uniformly dispersed in the matrix, while improving the interfacial interaction with the matrix. From a macroscopic point of view, the elastic modulus is a measure of the resistance of an object to elastic deformation. From a microscopic level, as long as it is a factor that can interfere with the strength of the inspection, it can affect the elastic modulus.

According to the data in Figure 10, after the nanoparticles are modified, the Young's modulus and shear modulus of the composite have increased to varying degrees. And according to Figure 10, it can be seen that with the increase of the graft ratio, there will be an increasing trend, and at the same time, the performance of the composite material will decrease with the increase of the drop of nanoparticles.

6. Conclusions

With the development of science and technology, people's production needs are increasing, and traditional computing power cannot meet the needs of production. Therefore, optimal computing has become a current research hotspot. With the gradual deepening of people's understanding of natural science, more and more materials are produced. The purpose of this paper is to study the structure optimization of carbon nanotubes based on swarm intelligence algorithm and evolutionary calculation. Although this paper discusses the structure and optimization calculation of carbon nanotubes, there are still shortcomings: when the single-objective particle swarm optimization algorithm solves high-dimensional complex problems, it is still easy to fall into the local optimal solution, and the convergence accuracy still has a large room for improvement.

Data Availability

No data were used to support this study.

Conflicts of Interest

There is no potential conflicts of interest in this study.

References

[1] K. K. Bhattacharjee and S. P. Sarmah, "Modified swarm intelligence based techniques for the knapsack problem," *Applied Intelligence*, vol. 46, no. 1, pp. 1–22, 2017.

[2] G. D. Ntouni, A. E. Paschos, and V. M. Kapinas, "Optimal detector design for molecular communication systems using an improved swarm intelligence algorithm," *Micro & Nano Letters*, vol. 13, no. 3, pp. 383–388, 2018.

[3] P. Gao, S. Wang, J. Lv, Y. Wang, and Y. Ma, "A database assisted protein structure prediction method via a swarm intelligence algorithm," *RSC Advances*, vol. 7, no. 63, pp. 39869–39876, 2017.

[4] W. Zhong, D. Tan, and X. Peng, "Fuzzy high-order hybrid clustering algorithm for swarm intelligence sets," *Neurocomputing*, vol. 314, no. NOV.7, pp. 347–359, 2018.

[5] S. Tabaghchi, "Priority-based task scheduling method over cloudlet using a swarm intelligence algorithm," *Cluster Computing*, vol. 23, no. 2, pp. 663–671, 2019.

[6] D. S. Son, J. M. Hyun, and J. R. Lee, "Optimization of the design of radar-absorbing composite structures using response surface model with verification using scanning free space measurement," *Composite Structures*, vol. 186, pp. 106–113, 2018.

[7] Z. Ahmadi, S. Ravandi, F. Haghghat, and F. Dabirian, "Enhancement of the mechanical properties of PAN nanofiber/carbon nanotube composite mats produced via needleless electrospinning system," *Fibers and Polymers*, vol. 21, no. 6, pp. 1200–1211, 2020.

[8] S. Lu, C. Zhao, and Z. Lu, "Real time monitoring of the curing degree and the manufacturing process of fiber reinforced composites with a carbon nanotube buckypaper sensor," *RSC Advances*, vol. 8, no. 39, pp. 22078–22085, 2018.

[9] W. Wang, J. Xu, Y. Zhang, and G. Li, "First-principles study of electronic structure and optical properties of silicon/carbon nanotube," *Computational Chemistry*, vol. 5, no. 4, pp. 159–171, 2017.

[10] L. Yan, L. Li, X. Ru et al., "Core-shell, wire-in-tube and nanotube structures: carbon-based materials by molecular layer deposition for efficient microwave absorption," *Carbon*, vol. 173, no. 11, pp. 145–153, 2021.

[11] R. A. Shutilov, V. L. Kuznetsov, and S. I. Moseenkov, "Vacuum-tight ceramic composite materials based on alumina modified with multi-walled carbon nanotubes," *Materials Science and Engineering*, vol. 254, pp. 114508.1–114508.10, 2020.

[12] D. Ma, Y. Wang, and L. Zhang, "Parameter optimization on the compressed polypyrrole/carbon nanotube composite electrode for capacitive deionization," *Desalination & Water Treatment*, vol. 85, pp. 84–91, 2017.

[13] Q. Zaib and F. Ahmad, "Optimization of carbon nanotube dispersions in water using response surface methodology," *ACS Omega*, vol. 4, no. 1, pp. 849–859, 2019.

[14] Y. Nakazato, D. Kawachino, Z. Noda, J. Matsuda, A. Hayashi, and K. Sasaki, "SnO₂-supported electrocatalysts on various conductive fillers for PECs," *ECS Transactions*, vol. 80, no. 8, pp. 897–906, 2017.

[15] E. S. Kudinova, E. A. Vorobyeva, N. A. Ivanova, V. V. Tishkin, and O. K. Alekseeva, "A magnetron sputtering method for the application of the Ni catalyst for the synthesis process of carbon nanotube arrays," *Nanotechnologies in Russia*, vol. 15, no. 11–12, pp. 715–722, 2020.

[16] D. Jean, S. Jessl, and K. Saeed, "Continuous flow chemical vapour deposition of carbon nanotube sea urchins," *Nanoscale*, vol. 10, no. 16, pp. 7780–7791, 2018.

[17] H. M. Park, S. M. Park, and S. M. Lee, "Automated generation of carbon nanotube morphology in cement composite via

- data-driven approaches,” *Composites*, vol. 167, pp. 51–62, 2019.
- [18] B. Peng, M. Annamalai, S. Mothes, and M. Schröter, “Device design and optimization of CNTFETs for high-frequency applications,” *Journal of Computational Electronics*, vol. 20, no. 6, pp. 2492–2500, 2021.
- [19] S. Dereli, “A novel approach based on average swarm intelligence to improve the whale optimization algorithm,” *Arabian Journal for Science and Engineering*, vol. 47, no. 2, pp. 1763–1776, 2022.
- [20] M. Ali, “Large-scale structural optimization using a fuzzy reinforced swarm intelligence algorithm,” *Advances in Engineering Software*, vol. 142, no. Apr., pp. 102790–102790.13, 2020.
- [21] X. Xue and Y. Wang, “Using memetic algorithm for instance coreference resolution,” *IEEE Transactions on Knowledge and Data Engineering*, vol. 28, no. 2, pp. 580–591, 2016.
- [22] A. Ali, “A proposed AI-based algorithm for safety detection and reinforcement of photovoltaic steel,” *Journal of Intelligent Systems and Internet of Things*, vol. 4, no. 1, pp. 41–55, 2021.
- [23] M. Z. A. A. Kadir, M. Algrnaodi, and N. Ahmed, “Optimal algorithm for shared network communication bandwidth in IoT applications,” *International Journal of Wireless and Ad Hoc Communication*, vol. 2, no. 1, pp. 33–48, 2021.